

Statistical properties of an incoherently driven nonlinear interferometer

P. D. Drummond,* K. J. McNeil, and D. F. Walls

Department of Physics, University of Waikato, Hamilton, New Zealand

(Received 8 February 1980)

A nonlinear interferometer driven with a partially coherent light field is analyzed. A limit on the fluctuations permissible in the driving field to observe bistability is calculated. For a Gaussian, broadband input field the transmitted radiation is shown to have enhanced intensity fluctuations.

I. INTRODUCTION

There has been considerable interest in optically bistable systems where a nonlinear interferometer is driven by a coherent driving field, resulting in a bistable behavior between the input and output fields.¹ The nonlinearity may either be due to a saturable absorber² or a dispersive effect.^{3,4} Recently Chrostowski and Zardecki⁵ considered the transmission of chaotic radiation through an absorptive medium inside a Fabry-Perot interferometer. These authors performed a numerical simulation of the system and showed that transmission of light with enhanced intensity fluctuations resulted. Previously Chrostowski and Krasinski⁶ had predicted that passing chaotic light through a saturable absorber increases the intensity fluctuations in the transmitted light. This effect has been observed in a recent experiment by Krasinski *et al.*⁷ who measured the intensity fluctuations in light produced by passing chaotic radiation through a saturable dye cell. The mechanism for this effect is clear. A saturable absorber will transmit large intensity fluctuations yet not transmit moderate intensity fluctuations, therefore enhancing the relative contribution of the large intensity fluctuations in the transmitted light. The possibility of producing light with intensity fluctuations greater than thermal light was first predicted by McNeil and Walls⁸ for the process of two-photon spontaneous emission.

In this paper we consider a medium consisting of N two-level atoms placed inside a Fabry-Perot cavity and driven with a partially coherent driving field. A limit on the fluctuations permissible in the driving field in order to observe bistability is calculated. For a purely chaotic driving field no bistability occurs. An analytic solution for the photon statistics of the transmitted light is obtained.

II. MODEL EQUATIONS

We wish to calculate the response of a high- Q interferometer with a cooperative fluorescent

medium (modelled as N two-level atoms) to an input field with Gaussian fluctuations. We therefore analyze a model in which the input field is a mixture of a resonant coherent part with a part having "thermal" (delta-correlated) statistics relative to the interferometer response time. It is still possible for the input to be reasonably monochromatic, even with a bandwidth greater than the interferometer bandwidth, so a single-mode calculation is reasonable, provided the interferometer resonances are sufficiently broadly spaced relative to the input bandwidth. In the limit of completely Gaussian input statistics, this can represent a model of a multimode laser input to the nonlinear interferometer. A diagrammatic representation of this system, and the relation between input bandwidth and cavity spacings, is given in Fig. 1.

We assume that because of the large fluctuations in the input field, the effect of quantum fluctuations (due to the nonlinear medium) is negligible. We may then describe the system by the semiclassical Maxwell-Bloch equations. The effect of quantum fluctuations has been studied by Lugiato⁹ and Drummond and Walls¹⁰ who show that these terms can be expressed in a power series in $1/N$. Thus, for large enough numbers of atoms, the quantum fluctuations will be negligible compared to the Gaussian input fluctuations. We assume we are in the region where the spatial mean-field approximation is applicable,¹¹ and we also assume homogeneous broadening and a traveling-wave (uniform) mode function. In this case the Maxwell-Bloch equations assume the form

$$\begin{aligned}\frac{\partial \alpha}{\partial t} &= -\kappa \alpha + gNj^- + E(t), \\ \frac{\partial}{\partial t} j^- &= -\gamma_{\perp} j^- + 2g\alpha j^*, \\ \frac{\partial}{\partial t} j^* &= -g(\alpha j^* + \alpha^* j^-) - \gamma_{\parallel}(j^* - j^0),\end{aligned}\tag{2.1}$$

where α is the amplitude of the cavity field mode, j^* and j^e are the expectation values of the atomic polarization and inversion, j^0 is the initial atomic

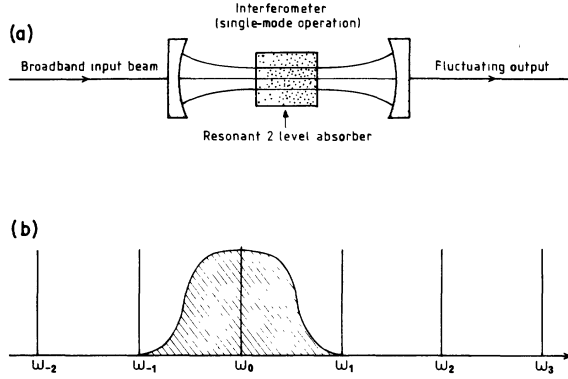


FIG. 1. (a) Schematic representation of the driven system. (b) Relation between the bandwidth of the driving field and the cavity mode spacings.

inversion, $E(t)$ is the driving field, and g is the atom-field coupling parameter. The cavity decay rate is κ and the atomic decay rates are γ_{\parallel} and γ_{\perp} . These equations have been used to describe optical bistability when $E(t)$ is a coherent driving field.^{2,4} We note that in actual experimental situations, inhomogeneous broadening can be significant. Further, a real laser beam has a Gaussian profile so that the above represents a very simplified treatment of the field mode function. In theory it is always possible to take such effects into account [c.f. Hassan *et al.*⁴ and Carmichael¹²].

For a high- Q cavity ($\kappa \ll \gamma_{\perp}$) we can adiabatically eliminate the atomic variables and obtain an equation for the field mode amplitude:

$$\frac{\partial}{\partial t} \alpha = E_0(t) + E_1(t) - \kappa \alpha - 2C \kappa \frac{\alpha}{1 + |\alpha|^2/n_0}, \quad (2.2)$$

where the cooperativity parameter $C = Ng^2/2\kappa\gamma_{\perp}$. Also, $n_0 = \gamma_{\perp}\gamma_{\parallel}/4g^2$, where g , the atom field coupling parameter, is defined by

$$g = |\langle 2 | \hat{d} | 1 \rangle| (\omega/2\hbar\epsilon_0 V)^{1/2},$$

and \hat{d} is the electric dipole operator. V is the quantization volume and N is the number of atoms, which are assumed to be distributed uniformly through the quantization volume. The condition for the spatial mean-field approximation to hold is $2c(1-R) \ll 1$, where R is the reflectivity of the cavity mirrors.

The input field may be divided into a coherent amplitude E_0 and a fluctuating amplitude E_1 . The fluctuating amplitude E_1 is assumed to have a thermal type of statistics (as might occur for a multi-mode source, or from thermal fluctuations induced in an optical transmission line). Therefore this radiation is regarded as broadband relative to the cavity bandwidth. However for simplicity, the

input is also regarded as filtered so that the intensity at the frequency of other Fabry-Perot modes is small relative to the principal excited mode.

Thus it is required that $\kappa \ll \Delta\omega_1 \ll c/2L$, where κ is the cavity bandwidth, $\Delta\omega_1$ is the input bandwidth, and c/L is the mode spacing for an interferometer of round trip length L . As the radiation is relatively broadband, it is regarded as Gaussian and delta-correlated on time scales comparable to the cavity reciprocal bandwidth:

$$\begin{aligned} \langle E_1(t)E_1^*(t') \rangle &= \Lambda \delta(t-t'), \\ \langle E_1(t) \rangle &= \langle E_1(t)E_1(t') \rangle = 0. \end{aligned} \quad (2.3)$$

The relative size of E_0 , Λ can be estimated for a given experiment as follows: The coherent input power (for perfect mode matching to a single resonant mode) is $L\hbar\omega|E_0|^2/c(1-R)$, where R is the mirror reflectivity and L is the round-trip path length. Similarly, the incoherent input power per unit frequency bandwidth is $L\hbar\omega\Lambda/c(1-R)$. In the case of a standard (nonabsorbing) interferometer, the coherent to incoherent transmitted power ratio would therefore be of order $|E_0|^2/\Lambda\kappa$.

III. BISTABILITY WITH A PARTIALLY COHERENT DRIVING FIELD

We introduce a probability distribution $P(\underline{\alpha})$ for the field amplitude $\underline{\alpha} = (\alpha, \alpha^*)$. Using standard techniques¹³ the stochastic differential equation (2.2) may be shown to be equivalent to the Fokker-Planck equation

$$\begin{aligned} \frac{\partial}{\partial t} P(\underline{\alpha}, t) &= \left[-\frac{\partial}{\partial \alpha} \left(E_0 - \kappa \alpha - 2C \kappa \frac{\alpha}{1 + |\alpha|^2/n_0} \right) \right. \\ &\quad \left. - \frac{\partial}{\partial \alpha^*} \left(E_0^* - \kappa \alpha^* - 2C \kappa \frac{\alpha^*}{1 + |\alpha|^2/n_0} \right) \right. \\ &\quad \left. + \Lambda \frac{\partial^2}{\partial \alpha \partial \alpha^*} \right] P(\underline{\alpha}, t). \end{aligned} \quad (3.1)$$

The steady-state solution of this equation may be found exactly, since the equation obeys the potential conditions.¹⁴ This solution is given by

$$\begin{aligned} P(\underline{\alpha}) &= \mathcal{N} \exp\left\{ (2/\Lambda) [-\kappa |\alpha|^2 + E_0 \alpha^* + E_0^* \alpha \right. \\ &\quad \left. - 2C \kappa n_0 \ln(|\alpha|^2 + n_0)] \right\} \\ &= \mathcal{N} P'(\underline{\alpha}), \end{aligned} \quad (3.2)$$

where \mathcal{N} is a normalization constant.

This distribution, plotted as a function of the real and imaginary part of $\underline{\alpha}$, has twin maxima in the bistable region, with each maximum being locally stable. This has been demonstrated by Schenzle and Brand,¹⁵ who together with Bonifacio *et al.*,¹⁶ obtained this solution for optical bistability for an equivalent situation where the thermal

fluctuations are dominant over the quantum fluctuations. This is completely different from the pseudopotential suggested by Gilmore and Narducci,¹⁷ which had a "sombbrero" shape with no bistability. The sombrero distribution is correct for the laser with an injected signal^{18,19} but not for the physically different situation embodied in optical bistability.

An important factor in the observation of optical bistability is the reduction of external fluctuations to the point that bistability can exist on relatively long time scales. Clearly the steady-state bimodal distribution is not bistable (as it is unique). The crucial point is that bistability occurs as a transient response. In order for it to occur, in an experiment, the tunneling or equilibration time should be much slower than the rise time of the input wave form and the detector response time. This tunneling time can be easily estimated in the case of the present model for external fluctuations because of the exact solutions obtained for a potential function [Eq. (3.5)].

In this situation, the well-known technique of Kramers²⁰ and Landauer and Swanson²¹ can be directly used to calculate the tunneling time. It is useful to rewrite the Fokker-Planck equation in the scaled variables:

$$\begin{aligned} x &= \alpha/\sqrt{n_0}, \quad y = E_0/\kappa\sqrt{n_0}, \\ D &= \Lambda/\kappa n_0, \end{aligned} \quad (3.3)$$

which leads to

$$\begin{aligned} \frac{1}{\kappa} \frac{\partial}{\partial t} P(\underline{x}) &= \left\{ -\frac{\partial}{\partial x} \left[y - x \left(1 + \frac{2C}{1 + |x|^2} \right) \right] \right. \\ &\quad - \frac{\partial}{\partial x^*} \left[y^* - x^* \left(1 + \frac{2C}{1 + |x|^2} \right) \right] \\ &\quad \left. + D \frac{\partial^2}{\partial x \partial x^*} \right\} P(\underline{x}), \end{aligned} \quad (3.4)$$

with steady-state solution

$$P(\underline{x}) = \mathfrak{N} \exp[-\phi(\underline{x})],$$

where

$$\phi(\underline{x}) = \frac{2}{D} [-|x|^2 + yx^* + y^*x - 2C \ln(1 + |x|^2)]. \quad (3.5)$$

The theory of Landauer and Swanson then predicts a tunneling time for a transition from a stable branch z_1 through a saddle point z_2 to another stable branch z_3 :

$$\tau \approx 2(\kappa D)^{-1} (e^{F_1 - F_2} + e^{F_3 - F_2})^{-1}. \quad (3.6)$$

Here the "free energies" F_1, F_3 are defined in terms of local potential integrals in the neighborhood of the stable branch:

$$F_{1,3} = -\ln \left(\int_{z_1, z_3} \exp[-\phi(\underline{z})] d^2z \right), \quad (3.7)$$

while the effective "free energy" F_2 at the saddle point is given by expanding the potential locally, relative to the principal direction (x):

$$\begin{aligned} \phi(x) &\approx \phi(z_2) - \frac{1}{2} a \Delta \operatorname{Re}(x) + \frac{1}{2} b \Delta \operatorname{Im}(x) \\ F_2 &\equiv \phi(z_2) + \frac{1}{2} \ln(b/a) \end{aligned} \quad (3.8)$$

An order of magnitude estimate of τ is simply $\ln \tau_{\max} \approx (\phi_2 - \phi_1)$, where ϕ_1, ϕ_2 are evaluated at the transition midpoint. For the case of $C \gg 1$ the threshold point is at $y = C, x = 1$ and the midpoint is for $y < C$. A calculation of the potential difference (near the transition midpoint) shows that this is of order C/D , as would be expected from Eq. (3.4). Now in order for bistability to be clearly observable, it is therefore necessary to have $C/D \gg 1$. In the case of $C \lesssim D$ the potential height of the saddle point is relatively small and the internal field responds by diffusion, without definite threshold behavior. This places an upper limit on the size of the background term for which bistability can be observed, namely, $\Lambda \ll \frac{1}{8} N \gamma_{\parallel}$. A numerical study of the effects of driving-field fluctuations on optical bistability has been made by Meystre.²²

It is an interesting problem to determine the behavior of the nonlinear interferometer when driven by an incoherent source with $\Lambda \geq \frac{1}{8} N \gamma_{\parallel}$. In this case, bistability does not occur. Instead, even for a completely Gaussian broadband driving field, a threshold still occurs at $\Lambda = \frac{1}{8} N \gamma_{\parallel}$. However, this is a completely different threshold from that for bistability; it is a threshold for a change in the correlation functions on statistics of the transmitted radiation. We consider this situation in the following section.

IV. PHOTON STATISTICS FOR A CHAOTIC DRIVING FIELD

We shall now consider the case where the incoherent component of the driving field is large. To simplify the analysis we assume a purely incoherent driving field and set $E_0 = 0$. In this case the steady-state, photon-number distribution given by Eq. (3.2) becomes a function solely of the photon number $R = |\alpha|^2$:

$$P(R) = \mathfrak{N}(R + n_0)^{-\epsilon} \exp(-R/\bar{n}), \quad (4.1)$$

where

$$\begin{aligned} \bar{n} &= \Lambda/2\kappa, \\ \epsilon &= 2Cn_0/\bar{n} = N\gamma_{\parallel}/2\Lambda. \end{aligned}$$

This distribution is a product of a Gaussian term characteristic of thermal light and an additional

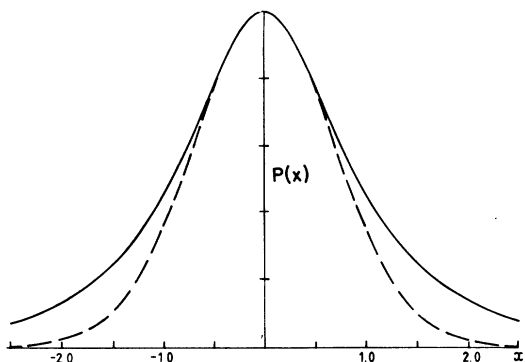


FIG. 2. Comparison of the distribution equation (4.1) with the Gaussian distribution $1/n_{\text{th}}e^{-R/n_{\text{th}}}$ (solid line, $e^{-0.1x^2}/(x^2+1)$); dotted line, e^{-x^2} . $\epsilon=1$, $n_0=1$, $\bar{n}=10$, $n_{\text{th}}=1$.

power-law term. A comparison with the Gaussian distribution for thermal light is shown in Fig. 2. The system is no longer bistable; however, a change in photon statistics occurs for a threshold value of the driving field, as may be seen from a calculation of the steady-state moments.

The distribution plotted in Fig. 2 is Eq. (4.1) with $\epsilon=1$, which gives a product of a Gaussian and a Lorentzian. It is these long Lorentzian-type tails in the distribution which gives large values for the moments.

These moments of the photon distribution may be calculated directly from Eq. (4.1). We initially compute the intensity moments of the un-normalized distribution:

$$\begin{aligned} I^{(j)} &= \pi \int_0^\infty R^j P'(R) dR \\ &= \pi \int_0^\infty R^j (R+n_0)^{-\epsilon} \exp(-R/\bar{n}) dR \\ &= \pi e^{-n_0/\bar{n}} \bar{n}^{j+1-\epsilon} \\ &\quad \times \sum_{k=0}^j (-z_0)^k \frac{j!}{(j-k)!k!} \Gamma(j+1-k-\epsilon, z_0), \end{aligned} \quad (4.2)$$

where Γ is the incomplete gamma function²³ and $z_0 = n_0/\bar{n} = \epsilon/2C$.

In order to obtain a physical understanding of the behavior of these moments we first consider the limit $\bar{n} \rightarrow \infty$. In this limit the behavior of the moments depends on the size of ϵ relative to the order of the moment. We consider two regions:

(i) $1+j < \epsilon$. For low moments the power-law term in the distribution function equation (4.1) dominates and

$$\begin{aligned} I^{(j)} &\simeq \pi \int_0^\infty \frac{R^j}{(R+n_0)^\epsilon} dR \\ &= \pi n_0^{(j+1-\epsilon)} \frac{\Gamma(j+1)\Gamma(\epsilon-j-1)}{\Gamma(\epsilon)}. \end{aligned} \quad (4.3)$$

(ii) $1+j > \epsilon$. For the higher moments the Gaussian term in the distribution function equation (4.1) dominates and

$$I^{(j)} \simeq \pi \int_0^\infty R^{j-\epsilon} e^{-R/\bar{n}} dR = \pi \bar{n}^{(j+1-\epsilon)} \Gamma(j+1-\epsilon). \quad (4.4)$$

The above results are true asymptotically for Λ , $N \rightarrow \infty$ with ϵ finite.

From the unnormalized moments we may calculate the n th-order correlation function of the radiation field as defined by Glauber²⁴:

$$G^{(n)} = I^{(n)} / I^{(0)^n}. \quad (4.5)$$

We again consider the limit $\bar{n} \rightarrow \infty$. In this case there are three distinct regions:

- (i) $j+1 < \epsilon$. $G^{(j)} \simeq n_0^j j! \Gamma(\epsilon-j-1) / \Gamma(\epsilon-1)$.
- (ii) $j+1 > \epsilon > 1$. $G^{(j)} \simeq \bar{n}^{(j+1-\epsilon)} n_0^{(\epsilon-1)} \Gamma(j+1-\epsilon) (\epsilon-1)$.
- (iii) $\epsilon < 1$. $G^{(j)} \simeq \bar{n}^j \Gamma(j+1-\epsilon) / \Gamma(1-\epsilon)$.

We note here that with decreasing ϵ , which corresponds to increasing Λ , each correlation function is uniformly increasing. However, there is a much greater rate of increase in the middle range for large values of C (because $\bar{n} \gg n_0$). Therefore this region can be regarded as the threshold. For the j th correlation function the threshold point is at

$$\bar{n}_{\text{thr}} = \frac{\Lambda_{\text{thr}}}{2\kappa} = \frac{2Cn_0}{(j+1)}. \quad (4.7)$$

For all the correlation functions the region (iii) gives a saturation behavior in which none of the correlations increase very rapidly. Instead the effective nonlinearity of the medium is reduced (as 50% of the atomic population are approaching inversion). The saturation point is at

$$\bar{n}_{\text{sat}} = \frac{\Lambda_{\text{sat}}}{2\kappa} = 2Cn_0 > \bar{n}_{\text{thr}}. \quad (4.8)$$

The scaling behavior of these correlation functions may be seen in Figs. 3 and 4. Finally we calculate the normalized correlation functions de-

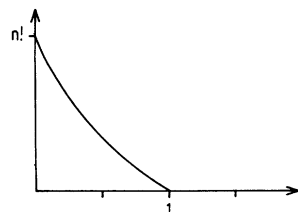


FIG. 3. $g^{(n)}(0) / (\bar{n})^n$ as a function of $2Cn_0/\bar{n}$ in the limit $\bar{n} \rightarrow \infty$.

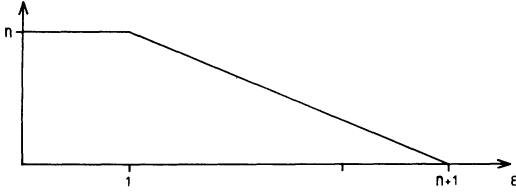


FIG. 4. $\ln [g^{(n)}(0)]/\ln(\bar{n})$ as a function of $2Cn_0/\bar{n}$ in the limit $\bar{n} \rightarrow \infty$.

finied by

$$g^{(j)}(0) = \frac{g^{(j)}(0)}{[g^{(1)}(0)]^j}. \quad (4.9)$$

In this case due to the normalization factor it is necessary to deal with four individual regions. These correspond to subthreshold, increasing $g^{(j)}(0)$, decreasing $g^{(j)}(0)$ and saturated behavior, respectively. In the asymptotic limit $\bar{n} \rightarrow \infty$ we have

(i) Subthreshold ($\epsilon > j + 1$):

$$\ln[g^{(j)}(0)] \approx 0.$$

(ii) Increasing ($j + 1 > \epsilon > 2$):

$$\ln[g^{(j)}(0)] \approx (j + 1 - \epsilon) \ln(\bar{n}/n_0). \quad (4.10)$$

(iii) Decreasing ($2 > \epsilon > 1$):

$$\ln[g^{(j)}(0)] \approx (\epsilon - 1)(j - 1) \ln(\bar{n}/n_0).$$

(iv) Saturated ($\epsilon < 1$):

$$\ln[g^{(j)}(0)] \approx 0.$$

$$g^{(j)}(0) = \frac{\sum_{k=0}^j (-z_0)^k \binom{j}{k} \Gamma(j+1-k-\epsilon, z_0) [\Gamma(1-\epsilon, z_0)]^{j-1}}{[\Gamma(2-\epsilon, z_0) - z_0 \Gamma(1-\epsilon, z_0)]^j}. \quad (4.13)$$

In Fig. 6 we show $g^{(2)}(0)$ as a function of $\Lambda/\Lambda_{\text{sat}} (= 1/\epsilon)$ for various values of C . The enhanced intensity fluctuations ($g^{(2)}(0) > 2$) in the region $1 < \epsilon < 3$ ($\frac{1}{3} < \Lambda/\Lambda_{\text{sat}} < 1$) are very apparent, as is the rapid saturation for $\Lambda/\Lambda_{\text{sat}} > 1$. Figure 6 is in good qualitative agreement with the numerical results of Chrostowski and Zardecki,⁵ Chrostowski and Krasinski,⁶ and the experimental work of Krasinski *et al.*⁷

Figure 7 shows the rapid increase in size of the $g^{(n)}(0)$ as n increases. As the parameter C is made larger this increase with n is so rapid that if a linear scale is used, for a given n , only $g^{(n)}(0)$ and $g^{(n+1)}(0)$ can be compared conveniently. Figure 7 shows $g^{(2)}(0)$ and $g^{(3)}(0)$ as functions of $\Lambda/\Lambda_{\text{sat}}$. In order to compare the $g^{(n)}(0)$ over a wider range of n , a logarithmic scale is required, and

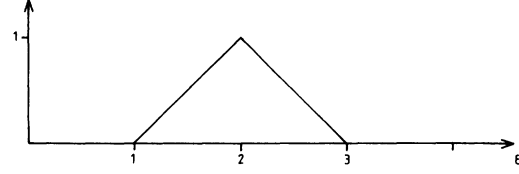


FIG. 5. $\ln [g^{(2)}(0)]/\ln(\bar{n})$ as a function of $2Cn_0/\bar{n}$ in the limit $\bar{n} \rightarrow \infty$.

In the asymptotic limit we therefore have all correlation functions with a maximum at

$$\bar{n} = Cn_0 = \gamma_{11}N/8\kappa. \quad (4.11)$$

The input field and value of the correlation function at the maximum will be approximately

$$\Lambda_{\text{max}} \approx 2C\kappa n_0, \quad (4.12)$$

$$[\ln g^{(j)}(0)]_{\text{max}} \approx (j-1) \ln C.$$

Thus there is a very close relationship between the cooperativity parameter and the degree of intensity correlation with a Gaussian input field (in the large C limit). However, this relation is expected to be only roughly true because the peak value occurs between the regions where approximations (ii) and (iii) are valid, and neither of these approximations will be correct there, except for very large values of C . In Fig. 5 we show how $g^{(2)}(0)$ scales in the asymptotic limit. The exact expressions for $g^{(j)}(0)$ are given by Eqs. (4.2), (4.5), and (4.9) yielding

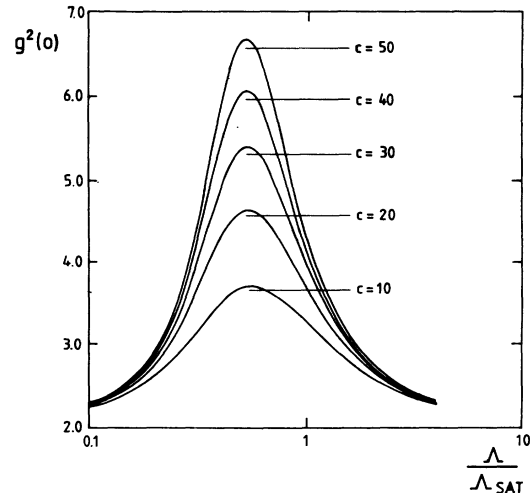


FIG. 6. $g^{(2)}(0)$ as a function of $\bar{n}/2Cn_0$ for $C = 10, 20, 30, 40, 50$.

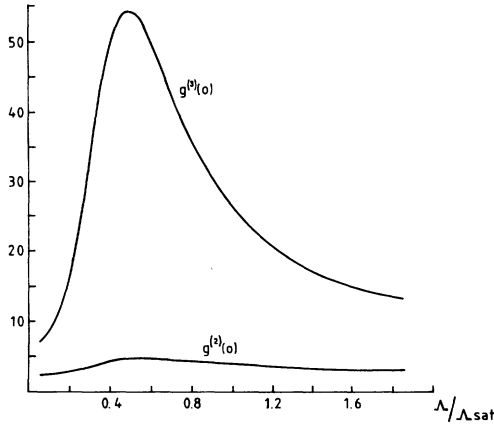


FIG. 7. $g^{(n)}(0)$ as a function of $\bar{n}/2Cn_0$ for $n=2$ and $n=3$. $C=20$.

this is shown in Fig. 8, where $\ln[g^{(n)}(0)]$ are plotted as functions of Λ/Λ_{sat} for various n .

The numerical computations showed that for $g^{(2)}(0)$ to obey relation (4.12), $C \geq 500$ is required. However, for the mean-field theory used here to be valid, the condition $2C(1-R) \ll 1$ must hold. For $C \approx 500$ this requires an interferometer reflectivity of $R > 0.999$, which would be difficult to obtain. In spite of this, even for $C < 500$ the numerical results do show a roughly linear increase of $[\ln g^{(2)}(0)]_{max}$ with $\log C$. For larger n values Eq. (4.12) is obeyed much more accurately, even for values of C as low as $C=20$ as in Fig. 8, which shows that $[\ln g^{(5)}(0)]_{max}$ and $[\ln g^{(6)}(0)]_{max}$ as predicted by Eq. (4.12) are very close to the exact values. Finally, we note that although the approximate relation for $[\ln g^{(j)}(0)]_{max}$ is not always valid, the numerical results show that the approximate expression for the position of the maxima, Λ/Λ_{sat}

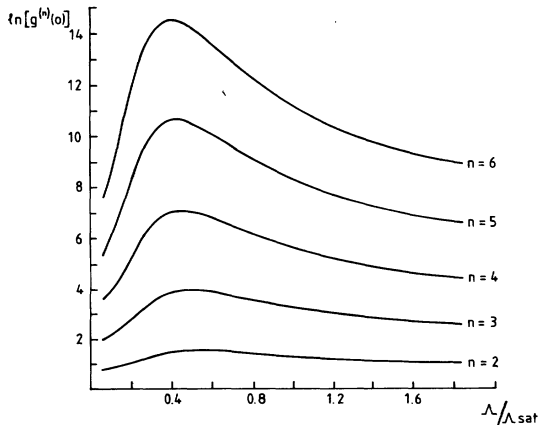


FIG. 8. $\ln[g^{(n)}(0)]$ as a function of $\bar{n}/2Cn_0$ for $n=2, 3, 4, 5, 6$. $C=20$.

$= \frac{1}{2}$, is in fact a good approximation for all the $g^{(n)}(0)$ calculated.

V. DISCUSSION

An analysis of a medium consisting of two-level atoms inside an interferometer shows that the statistical nature of the input radiation has a strong influence on the transmitted field. In the case of a mixed coherent and Gaussian driving field, the tunneling time in the bistable region can be estimated from a Fokker-Planck equation. When the intensity of the broadband Gaussian component exceeds a certain threshold, the tunneling time becomes sufficiently short to prevent bistability. In the case of a completely Gaussian broadband input with no coherent part, there is an enhancement of the output intensity fluctuations for intensities in a region about this same threshold value. It is easy to understand this behavior when one considers the saturable nature of the absorbing atoms in the cavity. Mathematically this is described by the term $\alpha/(1 + |\alpha|^2/n_0)$ in Eq. (3.1). For low driving fields there is no appreciable saturation, and the atoms behave simply as linear absorbers. The completely Gaussian driving field thus imposes a chaotic steady state with standard Gaussian fluctuations. As the driving field is increased saturation effects become important, and large intensity fluctuations are less likely to be absorbed. The resulting steady-state field thus exhibits relative fluctuations which become increasingly larger than Gaussian fluctuations as the driving is increased. At very high driving fields the atoms approach complete saturation and no longer absorb. The resulting steady state thus tends again to the Gaussian state dictated by the Gaussian driving field with a linear loss.

Depending on the cooperativity parameter C , higher-order correlation functions also exhibit increased values compared to those for thermal light. In the region of enhancement, we have $g^{(n)}(0) \approx C^{n-1}$. So for $n \leq C$ we obtain $g^{(n)}(0)$ values greater than the thermal light $g^{(n)}(0)$ value $n!$. $g^{(n)}(0)$ is a measure of the strength of the n -photon transition probability compared to a coherent field,²⁵ so in this case, for $n \leq C$, these probabilities are enhanced even further than for a Gaussian field. As n is increased past C the enhancement becomes less significant, and eventually $g^{(n)}(0)$ becomes less than the corresponding Gaussian value $n!$.

Since the onset of the enhancement region is different for each different order of correlation function, at low driving intensities the enhancement of $g^{(n)}(0)$ can be significantly higher than that of $g^{(n-1)}(0)$. Thus this system could have practical application as a correlation filter, creating a

driving field for multiphoton processes with the higher-order transition probabilities favored over lower-order multiphoton and single-photon processes. One limitation of this system is clearly the reduction in intensity due to dissipation in the nonlinear medium.

ACKNOWLEDGMENT

One of the authors (P.D.D.) wishes to acknowledge useful comments and criticism from Professor J. Eberly.

APPENDIX

We may also adopt a phenomenological master equation approach to describe the saturable absorber, using a probability function $P(n)$ for the number of photons in the cavity:

$$\begin{aligned} \frac{dP(n)}{dt} = & -\mathcal{G}(n+1)P(n) + \mathcal{G}nP(n-1) \\ & - \mathfrak{c}nP(n) + \mathfrak{c}(n+1)P(n+1) \\ & - \mathfrak{D}\frac{n}{1+n/n_0}P(n) + \mathfrak{D}\frac{n+1}{1+(n+1)/n_0}P(n+1). \end{aligned} \quad (\text{A1})$$

In this equation the terms in \mathcal{G} and \mathfrak{c} represent the coupling to the chaotic driving field. $\bar{n} = \mathcal{G}/(\mathfrak{c} - \mathcal{G})$ is the steady-state mean photon number for the empty cavity, and $\kappa = \mathfrak{c} - \mathcal{G}$ is the cavity damping constant. The terms in \mathfrak{D} describe the effect of the saturable absorber, with n_0 being the saturation photon number and \mathfrak{D} a constant proportional to the cooperativity parameter C . Equation (A1) may be derived from a set of equations describing the full atom-field system by adiabatically eliminating the atoms, as done, for example, by Scully and Lamb in their well-known derivation of the laser master equation.²⁶

Using the principle of detailed balance, the steady-state solution of Eq. (A1) is readily found to be

$$P(n) = P(0) \left(\frac{\mathcal{G}}{\mathfrak{c}}\right)^n \prod_{j=1}^n \left(1 + \frac{\mathfrak{D}}{\mathfrak{c}} \frac{n_0}{n_0+j}\right)^{-1}, \quad (\text{A2})$$

$$\langle n \rangle = P(0) \frac{n_0+1}{r\epsilon+n_0+1} rF(2, n_0+2, r\epsilon+n_0+2; r),$$

$$\langle n(n-1) \rangle = P(0) \frac{(n_0+1)(n_0+2)}{(r\epsilon+n_0+1)(r\epsilon+n_0+2)} r^2F(3, n_0+3, r\epsilon+n_0+3; r), \quad (\text{A5})$$

where $r = \bar{n}/(\bar{n}+1)$, $\epsilon = 2Cn_0/\bar{n}$. The second-order correlation function $g^{(2)}(0) = \langle n(n-1) \rangle / \langle n \rangle^2$ may then be calculated in a straightforward manner.

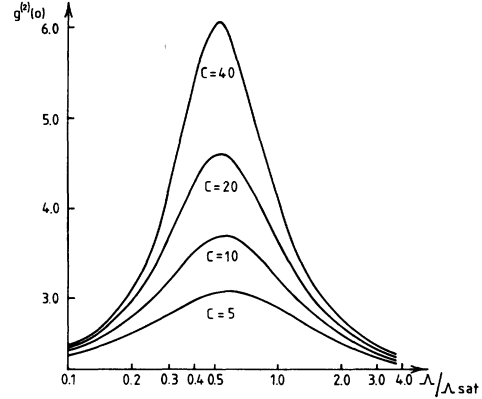


FIG. 9. $g^{(2)}(0)$ as a function of $\bar{n}/2Cn_0$ from the master equation approach of the Appendix; $C = 5, 10, 20, 40$.

where

$$P(0) = [F(1, n_0+1, n_0(\mathfrak{D}/\mathfrak{c} + 1) + 1; \mathcal{G}/\mathfrak{c})]^{-1}$$

where F is the hypergeometric function.

A simpler, approximate expression for $P(n)$ may be obtained using a method developed by Gragg *et al.*²⁷ Letting $\lambda_n = \mathcal{G}n$ and $\mu_n = [\mathfrak{c} + \mathfrak{D}(1 + n/n_0)]n$ we have in the case where $P(n)$ is a slowly varying function of n :

$$\begin{aligned} \frac{dP(n)}{dn} \simeq P(n+1) - P(n) &= \left(\frac{\lambda_n}{\mu_{n+1}} - 1\right)P(n) \\ &\simeq (\lambda_n/\mu_n - 1)P(n). \end{aligned} \quad (\text{A3})$$

This equation has the solution

$$P(n) = \mathfrak{N} [\mathfrak{c}(1 + n/n_0) + \mathfrak{D}]^{-\mathfrak{D}n_0/\mathfrak{c}^2} \exp(-ne/\mathfrak{c} - a), \quad (\text{A4})$$

where \mathfrak{N} is a normalization constant. $P(n)$ of Eq. (A4) has the same qualitative form as $P(R)$ for Eq. (4.1).

Since the distribution moments may be calculated without difficulty from the exact solution, Eq. (A2), we shall use this expression rather than Eq. (A4) to compute the moments. The mean number and first-factorial moment are readily found to be:

$g^{(2)}(0)$ is plotted in Fig. 9 as a function of \bar{n} for various values of \mathfrak{D} . The form of these curves agrees well with the results of Refs. 5-7.

- *Present address: Physics Department, University of Rochester, Rochester, New York 14627.
- ¹H. M. Gibbs, S. L. McCall and T. N. C. Venkatesan, *Phys. Rev. Lett.* **36**, 1135 (1976).
- ²R. Bonifacio and L. A. Lugiato, *Opt. Comm.* **19**, 172 (1976).
- ³J. H. Marburger and F. S. Felber, *Phys. Rev. A* **17**, 335 (1978).
- ⁴S. S. Hassan, P. D. Drummond, and D. F. Walls, *Opt. Comm.* **27**, 480 (1978).
- ⁵J. Chrostowski and A. Zardecki, *Opt. Comm.* **29**, 230 (1979).
- ⁶J. Chrostowski and J. Krasinski, *Phys. Lett.* **65A**, 326 (1978).
- ⁷J. Krasinski, C. Radzewicz, and J. Chrostowski, *Phys. Lett.* **70A**, 287 (1979).
- ⁸K. J. McNeil and D. F. Walls, *Phys. Lett.* **51A**, 233 (1975).
- ⁹L. A. Lugiato, *Nuovo Cimento* **50B**, 89 (1979).
- ¹⁰P. D. Drummond and D. F. Walls (unpublished).
- ¹¹P. Meystre, *Opt. Comm.* **26**, 277 (1978).
- ¹²H. J. Carmichael (unpublished).
- ¹³W. H. Louisell, *Quantum Statistical Theory of Radiation* (Wiley, New York, 1973).
- ¹⁴H. Haken, *Rev. Mod. Phys.* **47**, 67 (1975).
- ¹⁵A. Schenzle and H. Brand, *Opt. Comm.* **27**, 485 (1978).
- ¹⁶R. Bonifacio, M. Gronchi, and L. A. Lugiato, *Phys. Rev. A* **18**, 2266 (1978).
- ¹⁷R. Gilmore and L. Narducci, *Phys. Rev. A* **17**, 1747 (1978).
- ¹⁸P. D. Drummond, D. Phil. thesis, University of Waikato, 1979 (unpublished).
- ¹⁹L. A. Lugiato, *Lett. Nuovo Cimento* **23**, 609 (1978).
- ²⁰H. A. Kramers, *Physica* **7**, 284 (1940).
- ²¹R. Landauer and J. A. Swanson, *Phys. Rev.* **121**, 1668 (1960).
- ²²P. Meystre (unpublished).
- ²³I. S. Gradshteyn and I. M. Ryzhik, *Tables of Integrals, Series and Products* (Academic, New York, 1965).
- ²⁴R. J. Glauber, *Phys. Rev.* **130**, 2529 (1963).
- ²⁵P. Lambropoulis, C. Kikuchi, and R. K. Osborne, *Phys. Rev.* **156**, 1081 (1966).
- ²⁶M. O. Scully and W. E. Lamb Jr., *Phys. Rev.* **159**, 208 (1967).
- ²⁷R. F. Gragg, W. C. Schieve, and A. R. Bulsara, *Phys. Rev. A* **19**, 2052 (1979).